

Holstein polaron: the effect of multiple phonon modes

Lucian Covaci and Mona Berciu

Department of Physics and Astronomy, University of British Columbia, Vancouver, BC, Canada, V6T 1Z1

(Dated: February 5, 2008)

We generalize the Momentum Average approximations $MA^{(0)}$ and $MA^{(1)}$ to study the effects of coupling to multiple optical phonons on the properties of a Holstein polaron. As for a single phonon mode, these approximations are numerically very efficient. They become exact for very weak or very strong couplings, and are highly accurate in the intermediate regimes, *e.g.* the spectral weights obey exactly the first six, respectively eight, sum rules. Our results show that the effect on ground-state properties is cumulative in nature. In particular, if the effective coupling to one mode is much larger than to the others, this mode effectively determines the GS properties. However, even very weak coupling to a second phonon mode has important non-perturbational effects on the higher energy spectrum, in particular on the dispersion and the phonon statistics of the polaron band.

PACS numbers: 71.38.-k, 72.10.Di, 63.20.Kr

The coupling of electrons to phonons is a widely studied problem, because it leads to many interesting phenomena such as conventional superconductivity or the formation of polarons (composite objects comprised of an electron and the surrounding phonon cloud), important in several classes of materials. As a recent example, results from angle-resolved photoemission spectroscopy¹ (ARPES) have lead to new discussions about possible polaronic effects in high-temperature superconductors.²

Most theoretical studies of polaron properties are of the Holstein model with a single optical phonon mode,^{3,4} even though complex materials have many optical and acoustic phonons. The reason is that usually there is one optical mode to which the coupling is strongest, and one assumes that the effects of the other modes are perturbationally small. Also, the efficiency of various numerical methods⁴ such as exact diagonalization, diagrammatic Monte Carlo and variational methods employed for obtaining results in the intermediate coupling regime, where no exact solutions are known, suffers when the Hilbert space is enlarged by addition of multiple phonon modes.

Recently, the so-called Momentum Average (MA) analytical approximation^{5,6} has been shown to be highly accurate over most of the parameter space of the Holstein polaron problem, while requiring a numerically trivial effort irrespective of the dimensionality of the problem or the strength of the coupling. Moreover, its accuracy can be systematically improved.⁷ Such fast but accurate methods are useful for a quick survey of polaron properties in various regimes, which can then be followed by quantitatively more accurate, but significantly more time and resource consuming numerical simulations.

In this Rapid Communication we show how these approximations can be generalized to deal with multiple phonon modes, without loss of accuracy when compared to the single-mode results. This allows us to study easily the effects of multiple phonon modes on the polaron properties. As we show below, while for ground-state properties these effects are rather trivial, the higher-energy spectrum is significantly modified by additional phonon modes, even if coupling to them is perturbationally small.

The generalized Holstein Hamiltonian⁸ of interest is:

$$\mathcal{H} = \sum_{\mathbf{k}} \epsilon_{\mathbf{k}} c_{\mathbf{k}}^{\dagger} c_{\mathbf{k}} + \sum_{\mathbf{q}, \alpha} \Omega_{\alpha} b_{\mathbf{q}}^{\alpha \dagger} b_{\mathbf{q}}^{\alpha} + \sum_{\alpha, \mathbf{k}, \mathbf{q}} \frac{g_{\alpha}}{\sqrt{N}} c_{\mathbf{k}-\mathbf{q}}^{\dagger} c_{\mathbf{k}} (b_{\mathbf{q}}^{\alpha \dagger} + b_{-\mathbf{q}}^{\alpha}). \quad (1)$$

The first term describes a free electron on a d -dimensional lattice with N sites (its spin is irrelevant, thus the spin index is dropped), the second describes the optical phonon modes, and the third describes the electron-phonons couplings. Momenta sums are over the Brillouin zone.

We focus on finding the polaron's Green's function:^{5,6}

$$G(\mathbf{k}, \omega) = \langle 0 | c_{\mathbf{k}} \hat{G}(\omega) c_{\mathbf{k}}^{\dagger} | 0 \rangle, \quad (2)$$

where $\hat{G}(\omega) = [\omega - \mathcal{H} + i\eta]^{-1}$ is the usual resolvent ($\hbar = 1$) and $|0\rangle$ is the vacuum. The poles of this Green's function mark the polaron spectrum, and ground-state (GS) energies, effective masses, quasiparticle (qp) weights and average phonon numbers can then be calculated as discussed in Ref. 6. The spectral weight $A(\mathbf{k}, \omega) = -\frac{1}{\pi} G(\mathbf{k}, \omega)$ can also be directly compared against ARPES results.

To simplify notation, we first assume that there are only two phonon modes, and rename their operators as $b_{\mathbf{q}}$ (mode 1) and $B_{\mathbf{Q}}$ (mode 2). The generalization to more phonon modes is discussed below. We use repeatedly Dyson's identity $\hat{G}(\omega) = \hat{G}_0(\omega) + \hat{G}(\omega) \hat{V} \hat{G}_0(\omega)$, where $\hat{G}_0(\omega) = [\omega - \mathcal{H}_0 + i\eta]^{-1}$ corresponds to the non-interacting Hamiltonian, to generate an infinite system of coupled equations involving $G(\mathbf{k}, \omega)$ and the generalized Green's functions $F_{nm}(\mathbf{k}, \mathbf{q}_1, \dots, \mathbf{q}_n; \mathbf{Q}_1, \dots, \mathbf{Q}_m; \omega) = \langle 0 | c_{\mathbf{k}} \hat{G}(\omega) c_{\mathbf{k}_T}^{\dagger} b_{\mathbf{q}_1}^{\dagger} \dots b_{\mathbf{q}_n}^{\dagger} B_{\mathbf{Q}_1}^{\dagger} \dots B_{\mathbf{Q}_m}^{\dagger} | 0 \rangle$. Here $\mathbf{k}_T = \mathbf{k} - \mathbf{q}_T - \mathbf{Q}_T$ and $\mathbf{q}_T = \sum_{i=1}^n \mathbf{q}_i$, $\mathbf{Q}_T = \sum_{j=1}^m \mathbf{Q}_j$. Arguments identical to those of Ref. 7 show that all functions F_{nm} are proportional to $G(\mathbf{k}, \omega)$. It is thus more convenient to work with the rescaled functions $f_{nm}(\mathbf{k}, \{\mathbf{q}\}, \{\mathbf{Q}\}, \omega) = N^{(n+m)/2} F_{nm}(\mathbf{k}, \{\mathbf{q}\}, \{\mathbf{Q}\}, \omega) / G(\mathbf{k}, \omega)$, where we use the shorthand notation $\{\mathbf{q}\} \equiv \mathbf{q}_1, \dots, \mathbf{q}_n$, etc.

The solution has the standard form

$$G(\mathbf{k}, \omega) = [\omega - \epsilon_{\mathbf{k}} - \Sigma(\mathbf{k}, \omega) + i\eta]^{-1} \quad (3)$$

where the exact self-energy is given by

$$\Sigma(\mathbf{k}, \omega) = \frac{g_1}{N} \sum_{\mathbf{q}_1} f_{10}(\mathbf{k}, \mathbf{q}_1, \omega) + \frac{g_2}{N} \sum_{\mathbf{Q}_1} f_{01}(\mathbf{k}, \mathbf{Q}_1, \omega) \quad (4)$$

In terms of the new sets $\{\mathbf{q}\}_i \equiv \mathbf{q}_1, \dots, \mathbf{q}_{i-1}, \mathbf{q}_{i+1}, \dots, \mathbf{q}_n$ and $\{\mathbf{q}\}_{n+1} \equiv \mathbf{q}_1, \dots, \mathbf{q}_n, \mathbf{q}_{n+1}$, the functions f_{nm} are the solutions of the following recurrence relations:

$$f_{nm}(\{\mathbf{q}\}, \{\mathbf{Q}\}) = G_0(\mathbf{k}_T, \omega - n\Omega_1 - m\Omega_2) \left[g_1 \sum_{i=1}^n f_{n-1,m}(\{\mathbf{q}\}_i, \{\mathbf{Q}\}) + g_2 \sum_{j=1}^m f_{n,m-1}(\{\mathbf{q}\}, \{\mathbf{Q}\}_j) \right. \\ \left. + \frac{g_1}{N} \sum_{\mathbf{q}_{n+1}} f_{n+1,m}(\{\mathbf{q}\}_{n+1}, \{\mathbf{Q}\}) + \frac{g_2}{N} \sum_{\mathbf{Q}_{m+1}} f_{n,m+1}(\{\mathbf{q}\}, \{\mathbf{Q}\}_{m+1}) \right] \quad (5)$$

where the dependence on \mathbf{k}, ω is implicitly assumed for all f_{nm} , $G_0(\mathbf{k}, \omega) = (\omega - \epsilon_{\mathbf{k}} + i\eta)^{-1}$ is the free propagator, and $f_{00} \equiv 1$ by definition. These are the generalization of the equivalent single-mode equations of Ref. 7.

As for the single-mode problem, the MA⁽⁰⁾ approximation is obtained by replacing in the *r.h.s* of Eqs. (5)

$$G_0(\mathbf{k}_T, \omega - n\Omega_1 - m\Omega_2) \rightarrow \bar{g}_0(\omega - n\Omega_1 - m\Omega_2) \equiv \bar{g}_{nm}(\omega)$$

where the momenta averages

$$\bar{g}_0(\omega) = \frac{1}{N} \sum_{\mathbf{k}} G_0(\mathbf{k}, \omega)$$

are simple known functions.⁹ In terms of the functions

$$\mathcal{F}_{nm}(\omega) = \frac{1}{N^{m+n}} \sum_{\{\mathbf{q}\}, \{\mathbf{Q}\}} f_{nm}(\mathbf{k}, \{\mathbf{q}\}, \{\mathbf{Q}\}, \omega), \quad (6)$$

the momentum-independent MA⁽⁰⁾ self-energy is:

$$\Sigma_{MA^{(0)}}(\omega) = g_1 \mathcal{F}_{10}(\omega) + g_2 \mathcal{F}_{01}(\omega),$$

while the recurrence relations (5) take the simpler form $\mathcal{F}_{nm}(\omega) = \bar{g}_{nm}(\omega)[ng_1 \mathcal{F}_{n-1,m}(\omega) + mg_2 \mathcal{F}_{n,m-1}(\omega) + g_1 \mathcal{F}_{n+1,m}(\omega) + g_2 \mathcal{F}_{n,m+1}(\omega)]$ (of course, $\mathcal{F}_{00} = 1$).

Such recursive equations were previously solved in a different context by Cini *et al.*,¹⁰ but their solution cannot be generalized to more than two phonon modes, nor to MA⁽¹⁾ or higher levels (see below). We have found an alternative solution without these shortcomings. First, we rewrite these recurrence relations in matrix form:

$$V_k = A_k V_{k-1} + B_k V_{k+1}, \quad (7)$$

where the vector $V_k = (\mathcal{F}_{k,0}; \mathcal{F}_{k-1,1}; \dots; \mathcal{F}_{1,k-1}; \mathcal{F}_{0,k})^T$ contains all $k+1$ functions corresponding to a total of k phonons. A_k is a matrix of size $k+1 \times k$ with the only non-zero elements $(A_k)_{i,i} = (k-i)g_1 \bar{g}_{k-i,i}(\omega)$ and $(A_k)_{i+1,i} = (i+1)g_2 \bar{g}_{k-1-i,i+1}(\omega)$, $\forall i = 0, k-1$. Similarly, B_k is a matrix of size $k+1 \times k+2$ with the only non-zero elements $(B_k)_{i,i} = g_1 \bar{g}_{k-i,i}(\omega)$ and $(B_k)_{i,i+1} = g_2 \bar{g}_{k-i,i}(\omega)$, $\forall i = 0, k$. Dependence on ω is again implicitly assumed everywhere.

The solution is $V_k = M_k V_{k-1}$ with $V_0 = (1)$, where

$$M_k = \frac{1}{1 - B_k \frac{1}{1 - B_{k+1} \frac{1}{1 - \dots}} A_{k+1}} A_k. \quad (8)$$

is a continued fraction of matrices of increasing size. The self energy is $\Sigma_{MA^{(0)}}(\omega) = (g_1, g_2) V_1 = (g_1, g_2) M_1$. The continued fractions become convergent if truncated at levels $N \approx g_1^2/\Omega_1^2 + g_2^2/\Omega_2^2$, i.e. when one keeps contributions from f_{nm} corresponding to expected average numbers of phonons in the cloud. The generalization to more phonon modes is straightforward. V_k again contains all Green's functions with a fixed number of phonons, and the interaction links it only to $V_{k\pm 1}$. The matrices A_k and B_k have non-vanishing elements only on a number of diagonals equal to the number of modes. The dimension of these matrices increases now faster with increasing k , but it is still much less severe than the corresponding increase in numerical simulations. Also, note that the MA calculation is equally simple in any dimension, the only change being in the expression used for $\bar{g}_0(\omega)$.⁹

The analysis of the diagrammatic and variational meaning of MA⁽⁰⁾ and the sum rules it obeys, is identical to that for the single-mode case,^{5,6,7} and we do not repeat it. It again proves its accuracy over the entire parameter space, as long as $\Omega_i/t > 0.1, \forall i$. However, MA⁽⁰⁾ fails to correctly predict the polaron+one phonon continuum.^{6,11} To remedy this, we use MA⁽¹⁾ or a higher level approximation.⁷ In MA⁽¹⁾, Eqs. (5) for f_{01} and f_{10} are left unchanged, and the momentum average is made only for f_{nm} with $n+m \geq 2$. As shown in Ref. 7, MA⁽¹⁾ correctly predicts the polaron+one phonon continuum, besides giving small improvements in the accuracy of various other quantities, *e.g.* the number of exactly satisfied sum rules increases from six to eight. The derivation of $\Sigma_{MA^{(1)}}(\omega)$ follows identically that in Ref. 7, with the only difference that continued fractions there correspond to continued fractions of matrices [like in Eq. (8)] here. We will present the details of this straightforward derivation elsewhere,¹² instead focusing here on results.

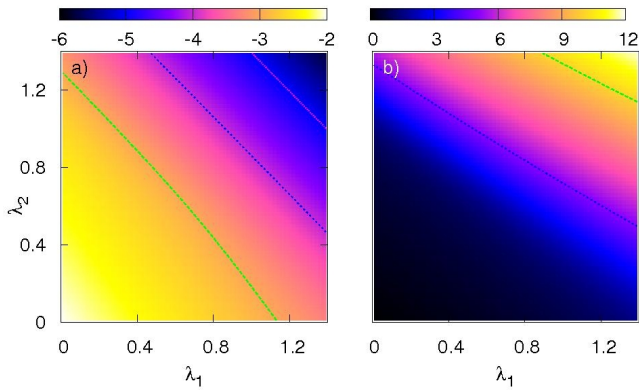


FIG. 1: (color online) (a) MA⁽¹⁾ GS energy and (b) $\ln(m^*/m)$, where m^* is the polaron effective mass, *vs.* coupling constants λ_1 and λ_2 , for $\Omega_1 = 0.7t$, $\Omega_2 = 0.3t$ and $d = 1$.

All results shown are for two phonon modes and $d = 1$, which suffices to uncover the essential new physics. Results for higher d and more phonon modes will be presented elsewhere.¹² We begin by discussing GS properties such as the energy E_{GS} and effective mass m^* , shown in Fig. 1 as functions of the effective couplings $\lambda_i = g_i^2/(2dt\Omega_i)$, $i = 1, 2$. Note that the qp weight is $Z_0 = m/m^*$, where m is the bare electron mass.⁶ The “equipotential” lines drawn show that E_{GS} is well described as a function of only $\lambda_{\text{eff}} = \sum_i \lambda_i$, whereas m^* is a function of $\sum_i \lambda_i/\Omega_i$. If $\Omega_i = \Omega$ for all modes, these can be proved to be *exact* results.¹² In the strong coupling limit one also expects $E_{GS} = -\sum_i g_i^2/\Omega_i$, $\ln Z_0 \propto -\sum_i \lambda_i/\Omega_i$, supporting the same conclusion. To a good extent the only effect of having $\Omega_1 \neq \Omega_2$ is to change the slope of the m^* “equipotentials” from the 45° found when $\Omega_1 = \Omega_2$, although some slight deviations from linearity are also seen in E_{GS} when either $\lambda_i \ll 1$.

We conclude that GS properties can be well understood in cumulative terms, for instance the energy is that of a polaron coupled to a single phonon with λ_{eff} . The crossover from large to small-polaron behavior is therefore expected when $\lambda_{\text{eff}} \approx 1$.^{3,4} As a result, it is possible to have small-polaron behavior even if each individual phonon mode is weakly coupled to the electron ($\lambda_i < 1$). However, in cases where one mode (say, mode 1) is indeed much more strongly coupled than all others, $\lambda_1 \gg \lambda_i$, $i = 2, \dots$, then $\lambda_{\text{eff}} \approx \lambda_1$ and one can, to a good extent, ignore the small cumulative effect from the other modes.

This conclusion, however, does not generally hold for higher-energy properties, as we show now. In Fig. 2 we plot the $d = 1$ spectral function $A(k, \omega)$ *vs.* k and ω . The effective coupling to the first mode, of frequency $\Omega_1/t = 0.7$, is kept constant to a fairly low value $\lambda_1 = 0.4$. In panel (a), coupling to the second mode, of energy $\Omega_2/t = 0.3$, is zero, so this is effectively a one-phonon problem. As expected, at low energies we see the polaron band, of width Ω_1 , followed above $E_{GS} + \Omega_1$ by the polaron+one-phonon continuum, and other features

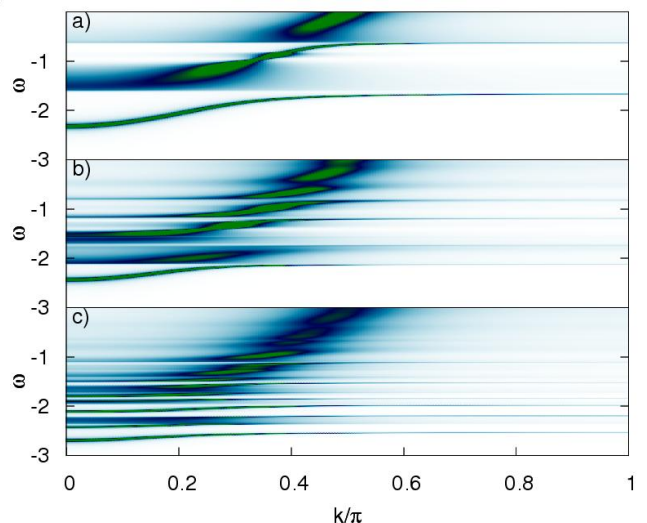


FIG. 2: (color online) $A(k, \omega)$ from MA⁽¹⁾ for $d = 1$, and for $\Omega_1 = 0.7t$, $\Omega_2 = 0.3t$, $\lambda_1 = 0.4$ and a) $\lambda_2 = 0.0$, b) $\lambda_2 = 0.2$, c) $\lambda_2 = 0.6$.

at even higher energies.^{3,4,7}

Addition of even very weak coupling to a second phonon mode changes things considerably, as shown in panel (b) for $\lambda_2 = 0.2$. If $\Omega_2 < \Omega_1$ (as chosen here), the polaron band width is changed to Ω_2 , even though the GS energy and effective mass are not much affected (see previous discussion). This significant change is not so surprising if one considers the origin of the polaron+one phonon continuum: it corresponds to states where one phonon is created far from the polaron. As a result, they interact little and the total energy is just the sum of the two. If there are several phonon modes, the continuum will be defined by the mode with the lowest frequency Ω_{min} , irrespective of whether this is the mode most strongly coupled to the electron or not. Because of this, the polaron band cannot be wider than Ω_{min} .

This interpretation is confirmed by phonon statistics, shown in Fig. 3. Here we plot average numbers N_1 and N_2 of phonons of either type in the polaron cloud, as a function of the polaron momentum k . These are calculated using the Hellman-Feynman theorem.^{6,13} Again, the coupling to the first mode is kept constant at $\lambda_1 = 0.4$. If $\lambda_2 = 0$ (+ symbols), we see that N_1 increases from a small value at $k = 0$ to just above 1 for $k > \pi/2$. This shows, as expected, that while around $k = 0$ the large-polaron is essentially similar to a free electron, for $k > \pi/2$ the largest contribution to the polaron comes from electron+one phonon states. Of course, $N_2 = 0$ in this case. As λ_2 is turned on but is still small ($\lambda_2 = 0.1, 0.3$, \times symbols) there is little change near $k = 0$, however the changes at higher momenta are dramatic: N_1 decreases by 1 whereas N_2 increases by 1 (note the different scales). This confirms that it is now the second type of phonon that controls the nature of the polaron at large k values, even though $\lambda_2 < \lambda_1$.

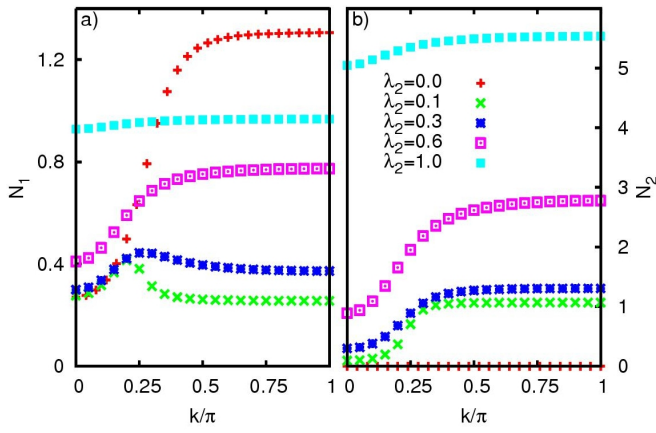


FIG. 3: (color online) Number of phonons of either type in the polaron cloud *vs.* λ_2 , for $\Omega_1 = 0.7t$, $\Omega_2 = 0.3t$ and $\lambda_1 = 0.4$.

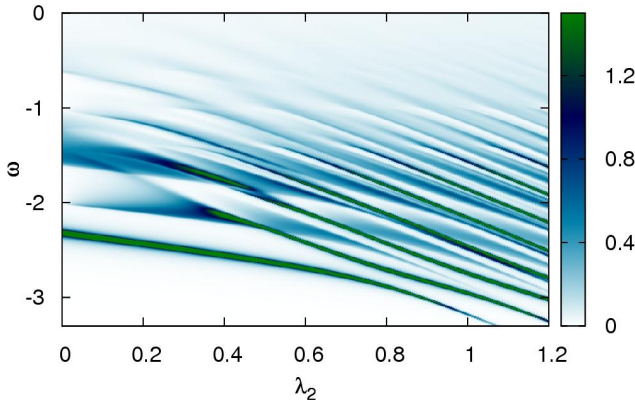


FIG. 4: (color online) $A(k=0, \omega)$ *vs.* ω and λ_2 , for $\Omega_1 = 0.7t$, $\Omega_2 = 0.3t$ and $\lambda_1 = 0.4t$.

Once $\lambda_2 > \lambda_1$, the second phonon completely dominates behavior. For $\lambda_2 = 0.6$ (square symbols) we have $\lambda_{\text{eff}} = \lambda_1 + \lambda_2 = 1$, and the polaron is in the crossover regime, whereas for $\lambda_2 = 1.0$, $\lambda_{\text{eff}} = 1.4$ the polaron is firmly in the small-polaron regime. In the latter case, we expect to see less and less k dependence, since the polaron cloud becomes limited to the site on which the

electron resides. This behavior is indeed observed for N_2 , but also for N_1 . This is because once the polaron is localized at a site (because of strong coupling to mode 2) it will automatically also shift the equilibrium position for mode 1 phonons at that site, resulting in the creation of a finite number of such bare phonons.

If there is only one phonon mode coupled to the electron, one can use ARPES data to extract its frequency Ω from the location of the “discontinuity” in the dispersion, at weak coupling, or from average distance between eigenstates at strong couplings, where the Lang-Firsov spectrum appears.¹⁴ The effective mass determines λ , so g can also be extracted. Our results show that this procedure is usually wrong in the case of multiple phonon modes, even if one expects coupling to one of them to be dominant. It only works if this particular mode also happens to have the lowest frequency, else one will underestimate its Ω and overestimate g . This point is clearly demonstrated in Fig. 4, which shows that the Ω_{min} phonon defines the location of the low-energy (not GS) features, irrespective of its coupling. Of course, one may hope to see the continua due to the other phonon modes (see also Fig. 2.c) and thus be able to identify their frequencies. This is probably unlikely, due to broadening in real data (note that temperature dependence would also be determined by the Ω_{min} phonon, not by the dominant one). Even if the Ω_i are identified, finding all g_i is generally impossible, unless we know that one dominates, and we know which one that is. The only simple case is if *all* phonons have roughly equal frequencies, when one can treat them as a single mode with coupling $g_{\text{eff}}^2 = \sum_i g_i^2$.

To summarize, we have found a generalization of the simple, yet accurate Momentum Average approximations to the problem of Holstein-type coupling to multiple phonon modes. Our results show that even perturbationally weak coupling to a second phonon can lead to essential changes of the spectral weight, if its frequency is less than that of the dominant phonon. In such cases, the simple way of extracting the electron-phonon coupling from ARPES data is likely to lead to wrong values.

Acknowledgments: We thank G. A. Sawatzky and F. Marsiglio for useful discussions. This work was supported by the A. P. Sloan Foundation, Cifar, NSERC and CFI.

¹ A. Damascelli, Z. Hussain, and Z.-X. Shen, Rev. Mod. Phys. **75**, 473 (2003).

² K. M. Shen *et al.*, Phys. Rev. Lett. **93**, 267002 (2004).

³ A. S. Alexandrov and N. F. Mott, *Polarons and Bipolarons*, (World Scientific, Singapore, 1995) and references therein.

⁴ For a recent review, see H. Fehske and S. A. Trugman, in *Polarons in Advanced Materials*, edited by A. S. Alexandrov (Canopus Publishing and Springer-Verlag GmbH, Bath, UK, 2007) and references therein.

⁵ M. Berciu, Phys. Rev. Lett. **97**, 036402 (2006).

⁶ G. L. Goodvin, M. Berciu and G. A. Sawatzky, Phys. Rev. B **74**, 245104 (2006).

⁷ M. Berciu and G. L. Goodvin, cond-mat/0705.4154.

⁸ T. Holstein, Ann. Phys. **8**, 325 (1959); *ibid* **8**, 343 (1959).

⁹ Expressions of $\tilde{g}_0(\omega)$ for nearest-neighbor hopping on simple cubic lattice in $d = 1, 2, 3$ are listed in Ref. 6.

¹⁰ M. Cini, J. Phys. **C19**, 429 (1986); M. Cini and A. D’Andrea, J. Phys. C **21**, 193 (1988).

¹¹ O. S. Barišić, Phys. Rev. Lett. **98**, 209701 (2007); M. Berciu, Phys. Rev. Lett. **98**, 209702 (2007).

¹² L. Covaci and M. Berciu, unpublished.

¹³ R. P. Feynman, Phys. Rev. **56**, 340 (1939).

¹⁴ I. G. Lang and Y.A. Firsov, Sov. Phys. JETP **16**, 1301 (1963).